Circulations between Mesoscale Convective Systems along a Cold Front

RICHARD H. JOHNSON, BARBARA D. MINER,* AND PAUL E. CIESIELSKI

Department of Atmospheric Science, Colorado State University, Fort Collins, Colorado

(Manuscript received 8 February 1994, in final form 28 July 1994)

ABSTRACT

A frontal squall line that passed over the central United States on 14–15 June 1985 consisted of several primary mesoscale convective systems (MCSs) with a prominent gap (several hundred kilometers wide) between two of them over central Kansas and Oklahoma. An upper-level jet streak crossed the front at right angles, with the jet exit region centered in the gap. Surface, upper-air, radar, and satellite data are used to examine conditions contributing to this squall-line gap.

All surface indicators (e.g., a sharp wind shift line and strong low-level moisture convergence) pointed toward the development of new deep convection in the gap. Computations of vertical velocity using sounding data showed that the low-level vertical motion was indeed upward there; however, strong subsidence existed aloft. The demarcation between subsidence aloft and ascent at low levels was near the 0°C level, where there was a concurrent inflow into the MCSs. A strong inversion existed near this level, which effectively capped vigorous congestus clouds that formed in the gap.

The circulations in the gap appeared to be first influenced by the upper-level jet and then the convection itself. Initial convection with the first MCS developed in the left-exit region of the jet. The second MCS evolved from initial cells that formed over strongly heated, higher terrain approximately 500 km to the southwest. The subsequent circulations between the MCSs—converging outflows aloft and at the surface, and diverging flow near the 0°C level—resemble those generated by gravity waves emanating from an MCS-like convective heat source. The gravity wave–induced subsidence aloft acted in opposition to the jet streak forcing, maintaining a strong cap and preventing deep convection in the squall-line gap. The distinction between highly broken squall lines (such as this one) and those with a nearly contiguous band of cells in the presence of strong low-level convergence appears to be related to the degree of convective inhibition in the environment and how it is modulated by a variety of processes including the convection itself.

1. Introduction

On 14–15 June 1985 during the Oklahoma–Kansas Preliminary Regional Experiment for STORM-Central (OK PRE-STORM), a cold front passed through the mesonetwork triggering two prominent mesoscale convective systems (MCSs). One storm formed in northeastern Kansas and another in the Oklahoma panhandle. Between the two (in the vicinity of Wichita, Kansas, hereafter referred to as IAB), deep convection did not develop despite strong low-level convergence along the cold front.[1] As will be seen, strong upper-level subsidence between the two MCSs was a likely contributor to the suppression of convection near IAB.

A case similar to this one has already been studied (Stensrud and Maddox 1988). In that situation two prominent MCSs developed on 23–24 June along an extensive line of convection from Iowa to the Oklahoma panhandle. The surface outflows from the MCSs collided over central Kansas in a region of conditional instability, leading forecasters to predict an outbreak of new storms; however, new convection did not occur. Computations of vertical velocity using sounding data in the region showed that while upward motion existed at low levels due to converging downdraft outflows, strong sinking occurred in the mid- to upper troposphere. This sinking created a strong capping inversion, which prevented new deep convection from forming. Stensrud and Maddox hypothesized that the subsidence aloft was a consequence of converging upper-level outflows from the two MCSs. A schematic illustration of this process is shown in Fig. 1. The opposing mesoscale flows on this day led to a particularly difficult forecast of the onset of convection.

[1] During PRE-STORM, National Weather Service forecasters at Wichita claimed that splitting of squall lines there was common, a phenomenon they referred to as the "Wichita gap." Realizing that many meteorologists tend to think that big storms miss them, we were skeptical of the claim of a preferential splitting of lines at Wichita. Some comment on this topic will be given later. There is certainly no evidence to indicate that Wichita is spared severe thunderstorm occurrences, as the 26 April 1991 Andover and other tornado outbreaks attest.

* Current affiliation: AWS/PMA, Scott Air Force Base, Illinois.

Corresponding author address: Dr. Richard H. Johnson, Department of Atmospheric Science, Colorado State University, Fort Collins, CO 80523.

© 1995 American Meteorological Society

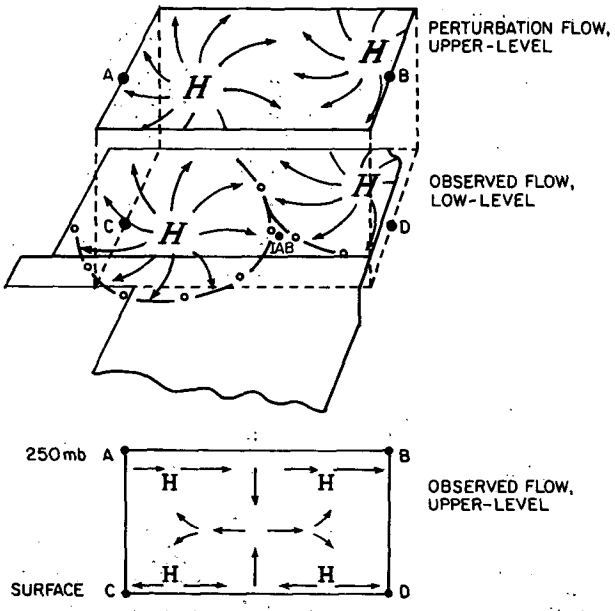

FIG. 1. Schematic of hypothesized perturbation upper-level and observed (or total) low-level flow patterns associated with two mesoscale convective systems on 23–24 June 1985 [adapted from Stensrud and Maddox (1988)]. Position of Wichita, Kansas (IAB), is indicated.

It is well known that new convection often develops along intersecting thunderstorm outflows, convergence lines, and fronts (Byers and Braham 1949; Simpson et al. 1980; Carbone 1982; Purdom and Marcus 1982; Weaver and Nelson 1982; Bluestein and Jain 1985; Wilson and Schreiber 1986). However, as noted by Stensrud and Maddox (1988), colliding surface outflows in a conditionally unstable atmosphere do not always produce new convection. In general, factors that inhibit new convective growth between existing convective elements are in part related to the way in which the environment responds to convection. Bjerknes (1938) argued that the environment of convection subsides, leading to a reduction in the buoyancy of convective updrafts. In a theoretical study Lilly (1960) concluded that most of the compensating subsidence in areas surrounding convective ascent occurs immediately adjacent to the updrafts. These findings led Fritsch (1975) and Fritsch and Chappell (1980) to propose that individual thunderstorms or MCSs could have overlapping regions of compensating descent, which would focus the sinking between systems, producing midlevel warming and surface mesolows. More recent studies have shown that the actual subsidence that occurs is achieved by gravity wave–like pulses that emanate from the heating and produce vertical motion in the environment (Szeto et al. 1988; Bretherton and Smolarkiewicz 1989; Nicholls et al. 1991). Mapes (1993) has shown that the influence of such waves is not always in a direction to suppress neighboring convection. For example, heat sources in the Tropics may promote new adjacent convection by the dispersion of gravity waves causing upward displacements at low levels. If there are no strong inhibiting effects, new convection can break out.

In general, however, the ability for new deep convection to form in the vicinity of existing convection along convergence lines or fronts appears to depend critically on processes occurring aloft. One complicating factor influencing such development is the common occurrence of upper-level jet streaks and their associated secondary circulations (Namias and Clapp 1949; Uccellini and Johnson 1979; Shapiro 1981). For example, Kocin et al. (1986) have shown that ageostrophic transverse circulations in the exit region of an upper-level jet streak can sufficiently destabilize the local environment to lead to an outbreak of deep convection in a matter of 3–6 h. However, in other areas, typically in jet right-exit regions, convection is often suppressed. When jet streak secondary circulations occur in concert with diabatically driven circulations, it becomes difficult to isolate the relative contributions of each.

In this study, data from the 14–15 June PRE-STORM squall line are analyzed to determine details of the circulations between two MCSs. Possible mechanisms for these circulations are explored. The data are unique in the sense that a dense network of soundings were available at 3-h intervals within the squall-line gap region; however, detailed circulations within the MCSs themselves could not be determined since the convection extended outside the sounding and radar networks.

2. Data analysis and procedures

a. Soundings

A discussion of the surface and upper-air networks employed in OK PRE-STORM is given in Cunning (1986). During the period of this study, special releases from 12 supplemental sites over Kansas and Oklahoma (Fig. 2) were made at 3-h intervals. Also indicated in this figure are the National Meteorological Center (NMC)–analyzed surface trough and frontal positions at 6-h intervals. The squall line developed along a cold front that tracked through the central United States on 14–15 June 1985.

Sounding data at three times (2100 UTC 14 June, 0000 and 0300 UTC 15 June) were interpolated to 25-mb intervals and resolved onto a $1/2° \times 1/2°$ grid using the objective analysis scheme of Barnes (1964). Vertical velocities were adjusted following O'Brien (1970) with the vertical velocity set to zero at 975 and 125 mb. The terrain slope is so small in the region of study that its effect on the vertical motion computation is negligible. In our use of the rawinsonde data, account is taken for both balloon drift and variable release times.

b. Surface data

Five-minute averages of temperature, moisture, wind, and pressure were obtained from a 50-km grid of National Center for Atmospheric Research (NCAR) Portable Automated Mesonetwork (PAM II) and National Severe Storms Laboratory (NSSL) Surface Automated Mesonetwork (SAM) stations (Johnson and Hamilton 1988). Pressures have been adjusted hydrostatically to 480 m (the mean elevation of the stations), and atmospheric tidal effects have been removed. Additional corrections to the pressures were made based on intercomparisons with surrounding National Weather Service (NWS) sites (Loehrer 1992).

c. Radar and satellite data

Low-level radar reflectivity data (0.5° elevation angle) from the NWS WSR-57 radars in the region have been prepared into composites using the analysis system located at the NSSL/Mesoscale Research Division laboratory in Boulder, Colorado. The satellite data used were from GOES-West, which was situated at 105°W during the experiment.

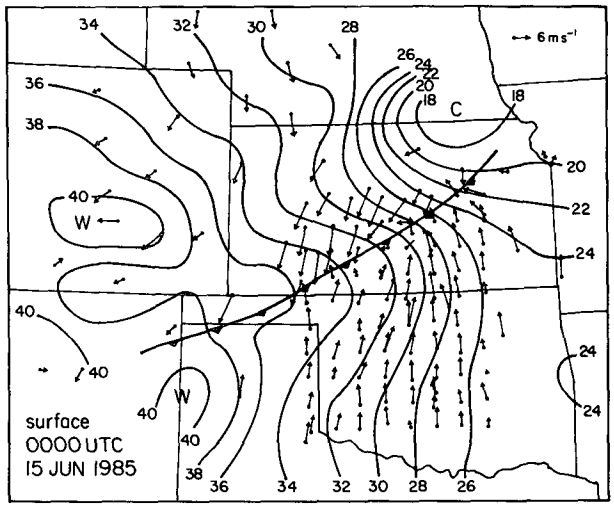

FIG. 3. Surface wind vectors (ground relative, scale on top right) and surface isentropes (°C) at 500 m (the approximate elevation at the center of the PRE-STORM network) at 0000 UTC 15 June 1985 (from Toth 1987). Double arrows at several sites are from collocated observing systems.

3. Synoptic, satellite, and radar overview

As shown in Fig. 2, a surface front extended through Kansas into southeastern Colorado at 0000 (all times are UTC on June 15; 0000 UTC = 1700 LST). The wind shift associated with the front can be seen in Fig. 3. Its position based on mesonet data is somewhat farther south than that analyzed by NMC in Fig. 2 (Toth 1987). The potential temperature θ adjusted to an elevation of 500 m (the approximate average elevation of the PAM and SAM stations, such that θ there nearly corresponds to surface temperature) shows both along- and cross-front gradients.[2] The cyclonic shear acting upon this gradient should induce a thermally direct ageostrophic circulation across the front (e.g., Shapiro 1981), a process that would be expected to assist convective development along the front. While cold advection was occurring north of the front, the cross-frontal temperature contrast changed little due to strong daytime heating. The cold pool in northeastern Kansas was associated with earlier convection in that region. Higher θ to the west was a result of daytime heating over elevated terrain.

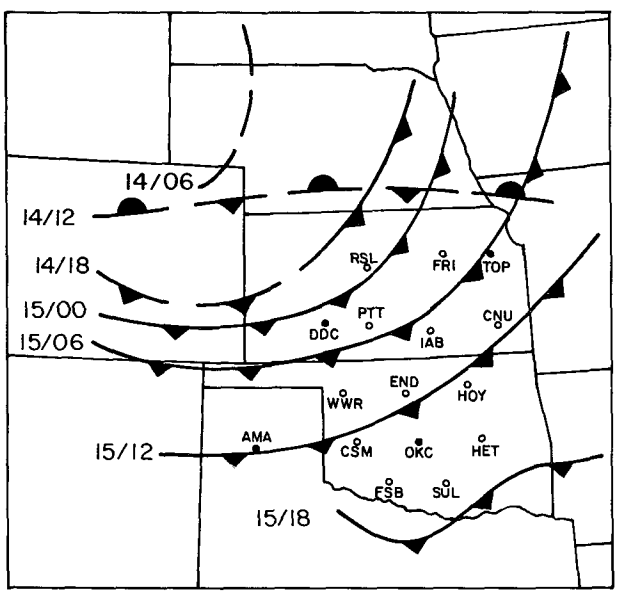

FIG. 2. NMC-analyzed frontal positions from 0600 UTC 14 June to 1800 UTC 15 June (from Toth 1987). Also indicated are PRE-STORM supplemental sites (open circles) and NWS sounding sites (closed circles) used in subsequent analyses.

The sharp wind shift associated with the front can also be seen at 850 mb over central Kansas (Fig. 4). The thermal field was similar to that shown at the surface in Fig. 3, and substantial low-level moisture was present south of the front. A short-wave trough at 500 mb was moving through the Midwest at this time (not shown).

At 300 mb (Fig. 5) a jet streak was advancing across the central plains with the left-exit region over northeastern Kansas. One of the primary MCSs along the front was in this location, consistent with the pattern of upper-level divergence and upward motion expected in

[2] Actually, the alongfront temperature gradient well exceeds the cross-front gradient, leading one to question the designation of this feature as a cold front by NMC. The existence of a wind shift line is unarguable, however.

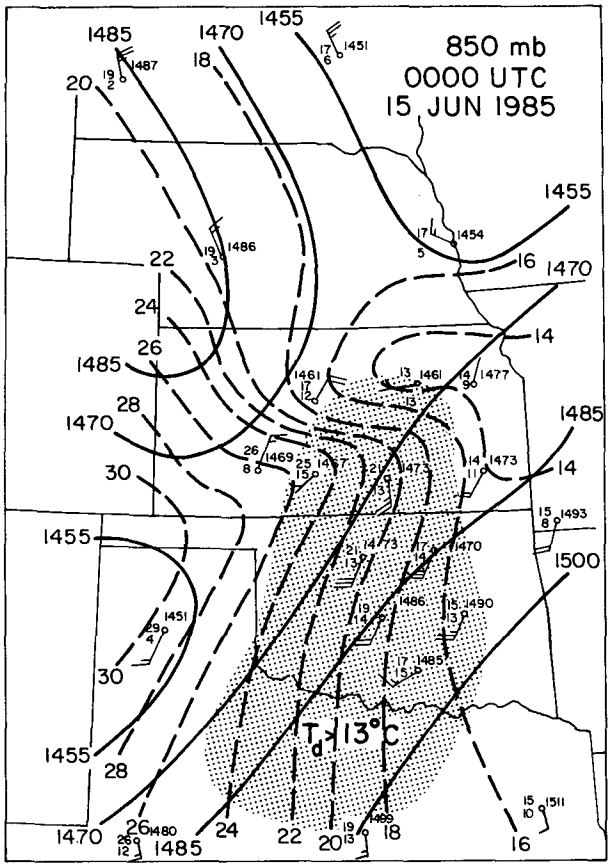

FIG. 4. Heights (m, solid) and isotherms (°C, dashed) at 850 mb at 0000 UTC 15 June 1985. Dewpoints greater than 13°C are shaded.

the left-exit region of an approximately straight jet streak (e.g., Namais and Clapp 1949; Uccellini and Johnson 1979). From jet streak dynamics alone, downward motion and a suppression of convection would be expected in the right-exit region over southwestern Kansas and western Oklahoma. Indeed, convection was initially suppressed in this location (Fig. 6). Weak cold advection evident along the jet axis (Fig. 5) should alter the expected secondary circulations slightly, shifting (a) the upward motion maximum farther off the axis in the left-exit region and (b) the downward motion maximum in the right-exit region toward the axis of the jet [Keyser and Shapiro (1986); see their Fig. 23]. Since the jet axis was in the region of the squall-line gap, these jet streak secondary circulations could offer at least a partial explanation for the initial pattern of convection in the region. Vertical cross sections of the vertical motion field normal to the jet axis will be presented later.

A review of the satellite imagery shows that a weak convective system crossed northern Kansas between 0600 and 1200 on 14 June 1985: its remnants can be seen in northeastern Kansas at 2030 (Fig. 6). At this time convection was breaking out in the Oklahoma panhandle and along the elevated Raton Mesa in southeastern Colorado (Fig. 7). Late in the afternoon (at 0000), new convection formed along the front in two locations—northeastern Kansas and the Oklahoma panhandle (Fig. 6). At 0130 the convection in northeastern Kansas expanded and moved to the southeast. Similarly, the convection in the Oklahoma panhandle increased in size and new cells formed toward the east and northeast along the front. However, convection did not form in the vicinity of IAB. By 0300 two prominent MCSs existed with a "gap" now southeast of IAB. At 0500 some merger of the upper-level clouds occurred as the MCSs continued to move to the southeast into Oklahoma; however, two distinct systems remained by 0800 and several hours beyond. According to Augustine and Howard (1988), the MCS to the northeast (MCS1) was classifiable as a mesoscale convective complex (MCC, Maddox 1980) by 0130 while the one to the southwest (MCS2) reached MCC proportions by 0300.

The low-level reflectivity field throughout this time period is shown in Fig. 8. At 0000 (Fig. 8a), MCS1 was only partially sampled but showed several scattered convective cores with lighter rainfall to the northeast. Only scattered cells were present over the Oklahoma panhandle in association with the development of MCS2. At this time a pronounced low pressure trough existed along the front, which was also an axis

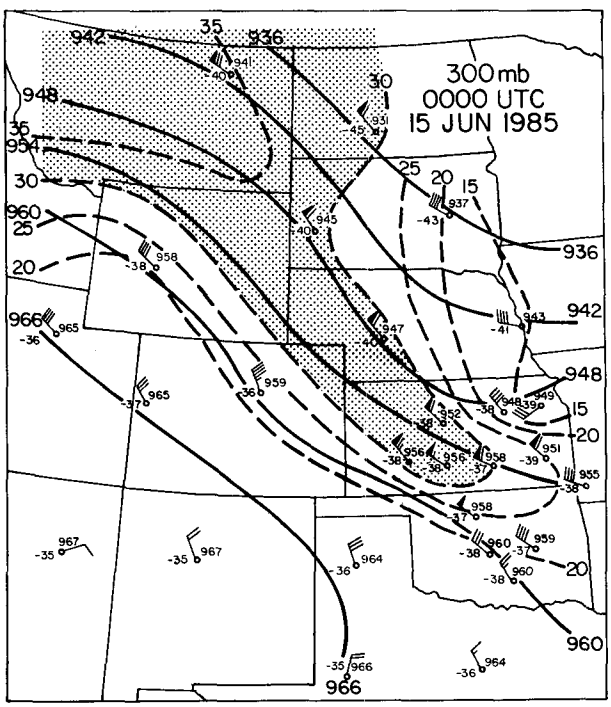

FIG. 5. Heights (dam, solid) and isotachs (m s^{-1}, dashed) at 300 mb at 0000 UTC 15 June 1985. Wind speeds in excess of 30 m s^{-1} are shaded.

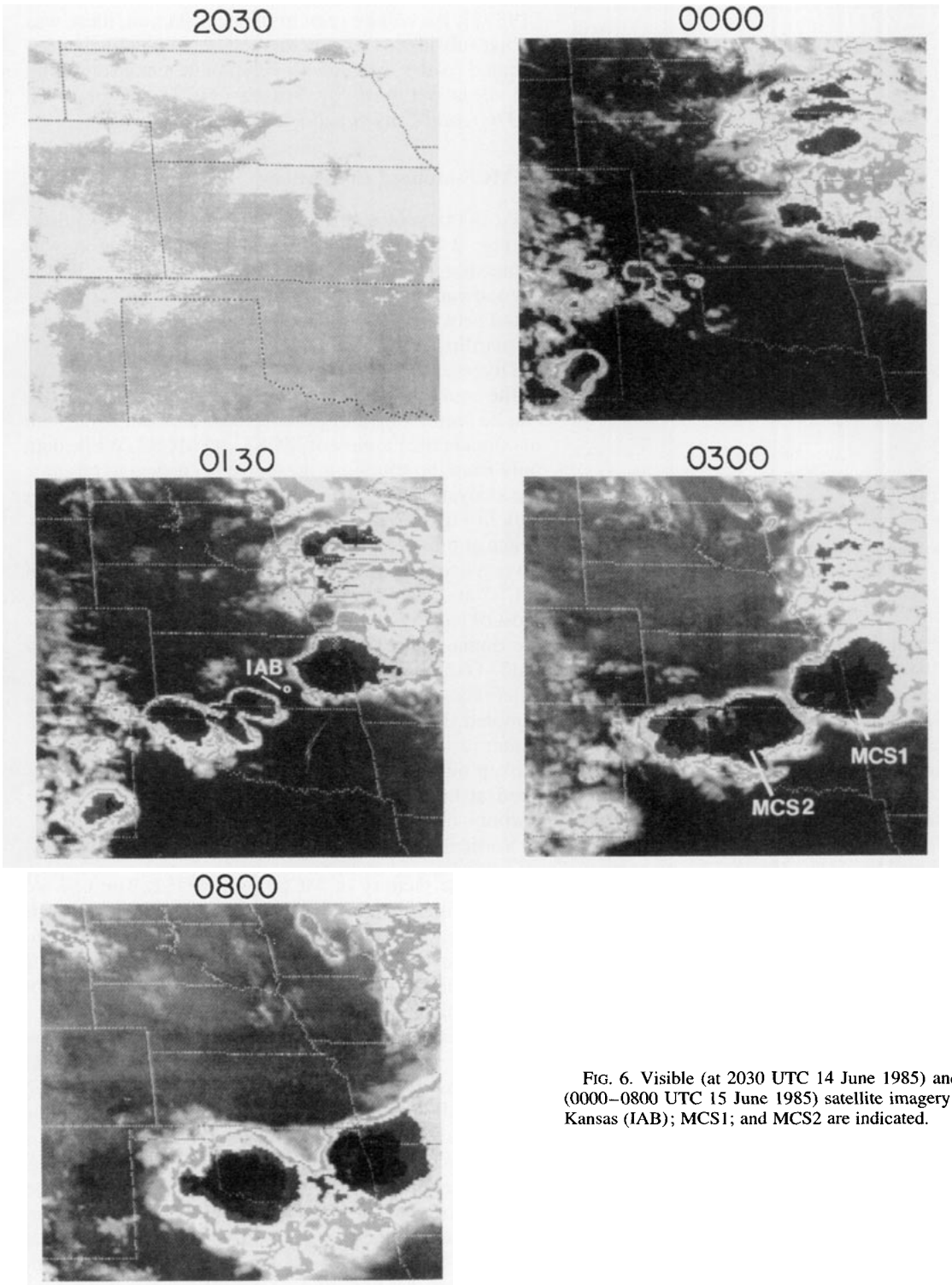

FIG. 6. Visible (at 2030 UTC 14 June 1985) and infrared (0000–0800 UTC 15 June 1985) satellite imagery. Wichita, Kansas (IAB); MCS1; and MCS2 are indicated.

of convergence of very warm, humid air. Over the next 2 h, convection associated with MCS1 and MCS2 built along the front toward IAB, but a 100–200-km gap was centered on IAB at 0200 (Fig. 8b). Other smaller gaps also existed in the line. By 0300 (Fig. 8c) the gap tended to close somewhat; however, there remained

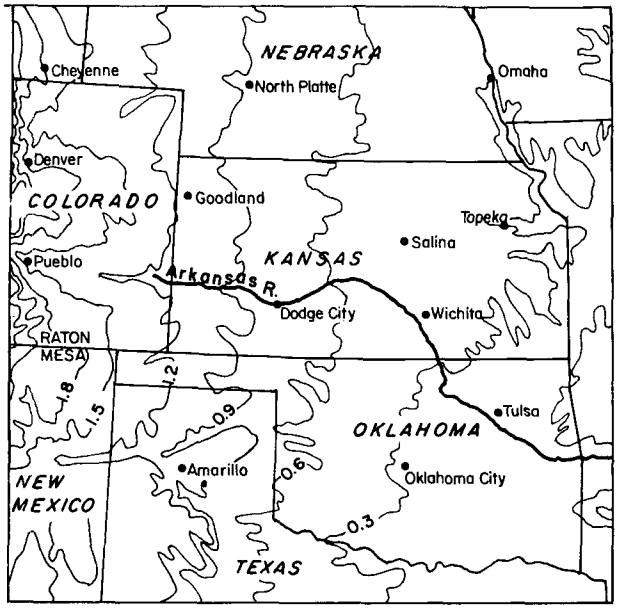

FIG. 7. Topographic map (elevations in kilometers) of PRE-STORM region.

two primary convective regions associated with MCS1 and MCS2, as also shown by the satellite data (Fig. 6). Downdraft outflows and surface mesohighs can be seen with each MCS, while a mesolow occurred ahead of the front between the two systems. The outflows from the two MCSs never expanded far enough toward each other to collide along the front. *The absence of colliding surface outflows in the 14–15 June case constitutes the primary difference between it and the 23–24 June case of Stensrud and Maddox (1988).* Finally, a mesohigh was also present in the region of light rainfall ahead of the front over Oklahoma.

Both the satellite and radar data at 0300 (Figs. 6 and 8c) indicate an extensive leading anvil associated with MCS2, whereas the anvil for MCS1 extended both to the east and northeast. This anvil structure is consistent with the pattern of advection of upper-level hydrometeors by the strong (25–30 m s^{-1}) northwesterly flow at 300 mb over western Kansas and the diffluent 300-mb flow over northeastern Kansas at this time (Fig. 5). During the period from 2100 to 0300 the front and squall line moved to the southeast rather slowly (~6 m s^{-1}) so that pronounced system-relative rear-to-front flow existed at upper levels of the storms.

Between 0300 and 0600, the speed of the front slowed to 4 m s^{-1} and the convection became somewhat disorganized, but two primary MCSs remained. However, at 0600 (Fig. 8d) MCS1 and MCS2 and their associated mesohighs had moved 100–200 km out ahead of the cold front, perhaps as a result of triggering of new convection on outflow boundaries. A prominent mesolow existed between the systems, as also occurred in the 23–24 June case [Fig. 12 of Johnson et al. (1989)]. As will be seen in the next section, there was strong subsidence aloft in this region, which likely contributed to the mesolow development, consistent with the ideas put forth by Fritsch (1975), Hoxit et al. (1976), and Fritsch and Chappell (1980).

4. MCS-induced circulations

At 0000, soundings were obtained from all stations in Fig. 2 except CSM. At 0300 the resolution was somewhat less since two critical ascents [at WWR (Woodward) and CNU (Chanute), see Fig. 2] terminated between 400 and 600 mb and soundings at AMA (Amarillo) and TOP (Topeka) were not made.

Divergence based on the 0000 surface observations at the sounding sites is shown in Fig. 9. Convergence can be seen along and just ahead of the cold front with maxima in the vicinity of MCS1 and MCS2. While data only from the sounding sites have been used to produce the analysis in Fig. 9, inspection of the surface mesonet data in Figs. 3 and 8a also suggests maximum convergence at these two locations. At 200 mb (Fig. 10), two divergence maxima are seen, one connected with MCS1 and the other in the area of MCS2. At this time, most of the convection in MCS2 was outside the sounding domain (Fig. 2) near the intersection of the Colorado–Oklahoma–Texas borders (Fig. 6), so the circulations associated with MCS2 were only partially sampled. It is intriguing to note a 200-mb divergence center just east of MCS2 where convection had not yet broken out at 0000. Within 1 h, an intense cell developed at this location, which grew to significant proportions by 0200 (Fig. 8b).

Vertical motion at 700 mb (Fig. 11) was upward all along and ahead of the front at 0000, with primary maxima in the vicinity of MCS1 and MCS2. The upward vertical motion and abundant moisture at low levels (Figs. 4 and 8a) would be expected to favor new convective development all along the front; however, at a slightly higher level (500 mb, Fig. 12), a region of downward motion can be seen near Wichita (IAB).

To examine the relationship of the downward motion at 500 mb over Wichita to the flow above, a vertical cross section has been constructed from the averaged gridded fields in 100-km-wide bands along the front intersecting MCS1 and MCS2 or their precursor storms (center axes of bands shown in Fig. 9). The first of these sections (Fig. 13) is shown at a time 3 h earlier (at 2100 UTC) to explore the possible role of the upper-level jet in convective development. This section extends from near the axis of the jet to the left-exit region. The vertical motion field shows ascent throughout most of the troposphere, except on the extreme left edge (near the jet axis). This pattern of motion is qualitatively consistent with that expected in the exit region of a jet with cold advection (Keyser and Shapiro 1986) as described earlier. It favors the development of convection from RSL (Russell) to the northeast; however, con-

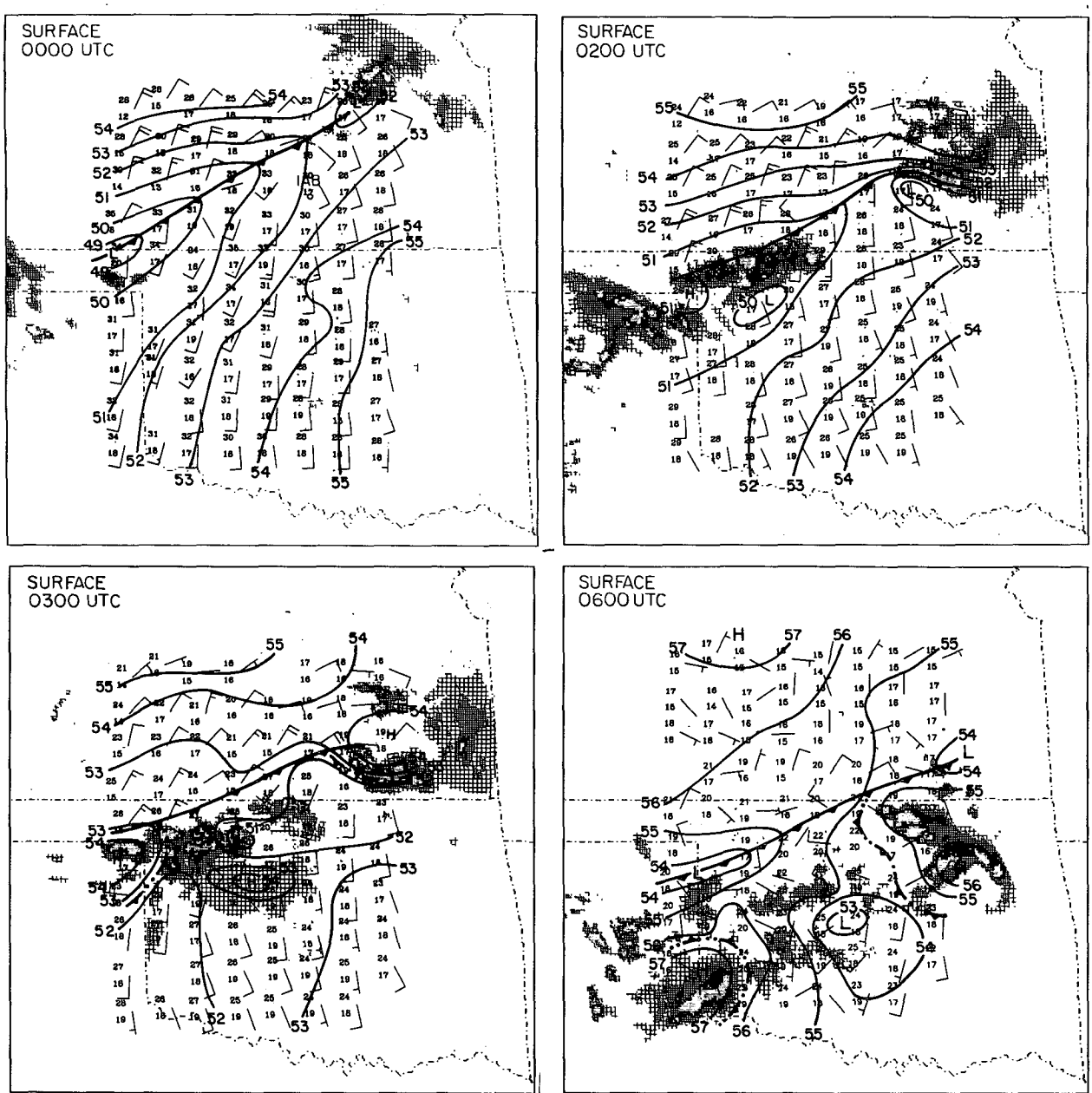

FIG. 8. Surface pressures adjusted to an elevation of 480 m (54 = 954 mb, etc.), base-scan radar reflectivities, frontal positions (double-dot dashed lines refer to gust fronts), surface temperature and dewpoint (°C), and wind from mesonet stations at (a) 0000, (b) 0200, (c) 0300, and (d) 0600 UTC 15 June 1985. Reflectivity thresholds are 16, 25, 40, and 49 dBZ.

vection actually developed much farther to the northeast (FRI and eastward), as evident from Figs. 6 and 9.

At 0000, a longer portion of the front intersected the sounding domain, so a longer cross section could be constructed (Fig. 14). This cross section is perpendicular to and approximately centered on the 300-mb jet axis at this time. Referring first to the divergence field (Fig. 14a), strong divergence centers near 200 mb occurred over MCS1 and MCS2. However, between these centers, in the entire layer from 500 to 150 mb, strong convergence was observed over IAB. At low levels, there was a another convergence maximum near 900 mb over IAB. Between these two was a strong midtropospheric divergence maximum centered near 600 mb. Finally, a divergence center due to downdrafts can be seen at the surface in the area of MCS1.

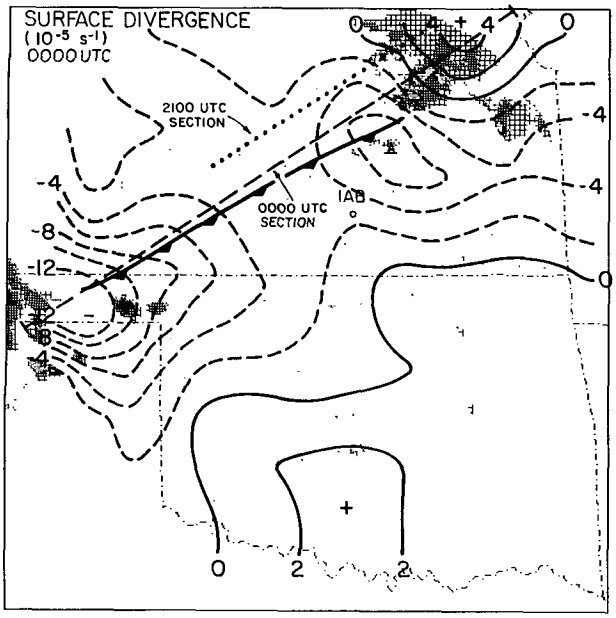

FIG. 9. Surface divergence (10^{-5} s^{-1}) and radar reflectivity at 0000 UTC 15 June 1985. Dashed straight line segment is center axis of cross section in Fig. 13. Reflectivity thresholds are 16, 25, 40, and 49 dBZ.

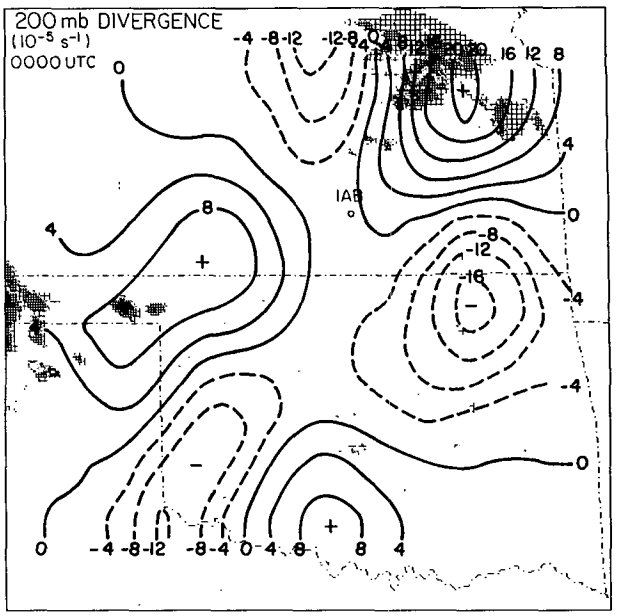

FIG. 10. As in Fig. 9 except at 200 mb.

Although the full three-dimensional wind field was used to compute the divergence field in Fig. 14a, the importance of MCS circulations in contributing to it can be viewed by plotting the perturbation wind component (deviation from the mean) in the plane of the section. These results (Fig. 14b) show converging perturbation flows aloft from MCS1 and MCS2 as well as converging flows near the surface in the lowest 1.5 km. In contrast, strong perturbation flow existed *toward* both MCS1 and MCS2 between 600 and 700 mb, very close to the T_w = 0°C level.[3] (For reference, the left-hand edge of Fig. 14 intersects the more extensive convection in MCS2 on the extreme left edge of Fig. 8a.).

Numerous studies have reported strong convergence into MCSs in the midtroposphere. Maximum convergence near 700 mb into mature MCCs has been found by Maddox (1983). Peak convergence near the 0°C level has been commonly observed in stratiform precipitation regions in both the Tropics (Gamache and Houze 1982; Johnson 1982; Houze and Rappaport 1984; Chong et al. 1987; Mapes and Houze 1993) and midlatitudes (Ogura and Liou 1980; Smull and Houze 1987; Stensrud and Maddox 1988; Gallus and Johnson 1991). It is ascribed to the cooling effects of melting and evaporation at low levels and heating aloft, which induce a mesolow and perturbation inflow into the system near the 0°C level (Leary and Houze 1979; Szeto et al. 1988; Biggerstaff and Houze 1991; Gallus and Johnson 1992). Circulations closely resembling the perturbation u field in Fig. 14b have been obtained by Nicholls et al. (1991) by investigating the linear response of the atmosphere to heating distributions char-

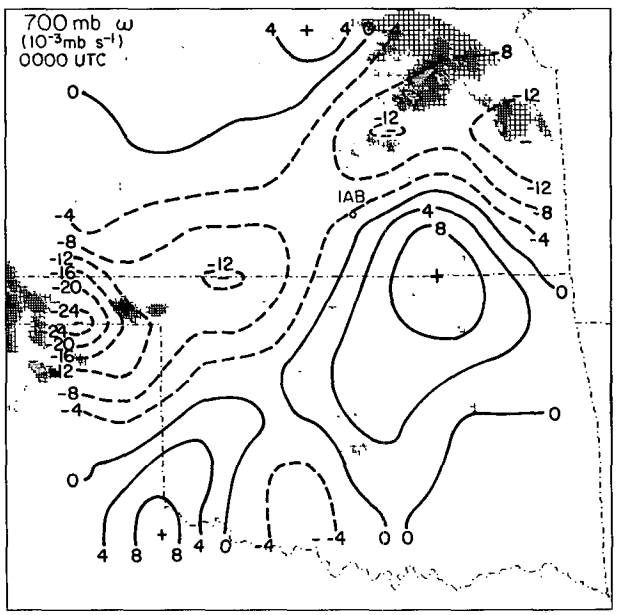

FIG. 11. Vertical p velocity (10^{-3} mb s^{-1}) and radar reflectivity at 700 mb at 0000 UTC 15 June 1985. Reflectivity thresholds are 16, 25, 40, and 49 dBZ.

[3] Here and in subsequent figures the wet-bulb temperature T_w = 0° level is denoted in order to represent a melting level both inside and outside precipitation regions.

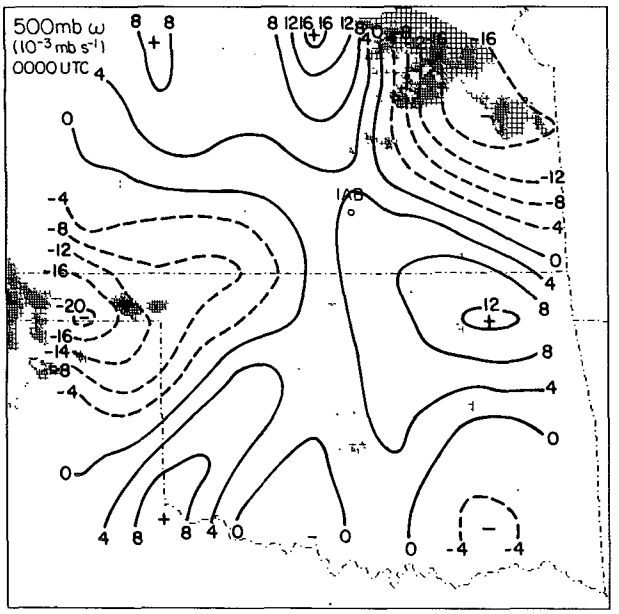

FIG. 12. As in Fig. 11 except at 500 mb.

acteristic of MCSs. It is found that the stratiform contribution to the total heating (heating aloft and cooling at low levels) yields a transient disturbance that propagates away from the heat source, having a vertical motion couplet characterized by sinking aloft and rising motion at low levels. This disturbance induces midtropospheric inflow toward the source and upper- and lower-tropospheric outflows away from the source.

Vertical motion along the front is shown in Fig. 14c. Upward motion was present in both MCS1 and MCS2, with the peak in MCS1 at a higher level than in MCS2. This difference is consistent with the fact that MCS1 was a mature system at this time while the portion of MCS2 sampled by the sounding network was still developing (Figs. 6 and 8). However, between the two MCSs, significant changes occurred over a 3-h period. While rising motion was present just east of the jet core at 2100 (Fig. 13), downward motion had developed above 600 mb in that location by 0000 (Fig. 14c). However, upward motion persisted below 600 mb.

Comparison of Fig. 14c with Figs. 14a and 14b suggests that the subsidence over IAB can be explained in terms of convergence aloft of the upper-level outflows from the two MCSs, as hypothesized by Stensrud and Maddox (1988) for the 23–24 June case. Indeed, this seems to be the case here too; however, it is interesting to note from satellite data (Fig. 6) that the actual cirrus anvils were not even approximately close to each other at 0000. This wide separation between the cirrus clouds (which are advected) and the perturbation outflows suggests that processes acting on a timescale faster than advection are accounting for subsidence in the gap. It is unlikely that jet streak dynamics can account for the subsidence there since the subsidence axis (Fig. 14c) is shifted approximately 200 km to the east of the jet axis, a pattern not expected for the left-exit region of the jet streak.

Since jet streak circulations do not appear to be a plausible explanation for the rapidly developed subsidence in Fig. 14c, another mechanism must be sought. One possibility involves convectively generated gravity waves (Nicholls et al. 1991; Mapes 1993). Mapes (1993) shows that a heat source can excite gravity waves that yield *net vertical displacements* in a fluid following their passage. He argues that such disturbances are best referred to as "buoyancy bores" because of the important irreversible (nonoscillatory) flows that respond to the net heating. Both the first internal or $n = 1$ mode (which moves the fastest) and the $n = 2$ mode produce subsidence in the upper troposphere as the waves propagate away from the source [Figs. 3 and 5 of Nicholls et al. (1991) and Fig. 3 of Mapes (1993)]. For an atmosphere at rest, the speed of an internal mode n is given by

$$c = \frac{NH}{n\pi}, \tag{1}$$

where N is the Brunt–Väisälä frequency and H is the fluid depth. Using an average N from 2 to 8 km of 1.1 $\times 10^{-2}$ s^{-1} and $H = 12$ km, then for $n = 2$, $c = 21$ m s^{-1}, half the speed of the first internal mode. The important point is that subsidence associated with these waves outruns the actual outflow of cloud-filled anvil air masses. For the two MCSs in this case that were developing about 600 km apart, it would take approximately 4 h for the subsidence from the $n = 2$ mode to reach the midpoint. It appears from Fig. 6 that sufficient convection was developing in MCS1 and MCS2 4 h

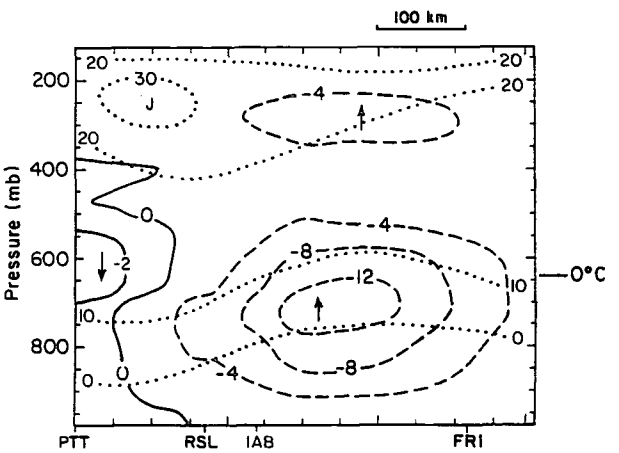

FIG. 13. Southwest–northeast vertical cross section along line segment in Fig. 9 of vertical p velocity (10^{-3} mb s^{-1}) at 2100 UTC 14 June 1985. Isotachs (m s^{-1}) for flow perpendicular to the plane of the section are indicated by dotted lines (J marks jet core). Wet-bulb temperature $T_w = 0$°C level is also shown.

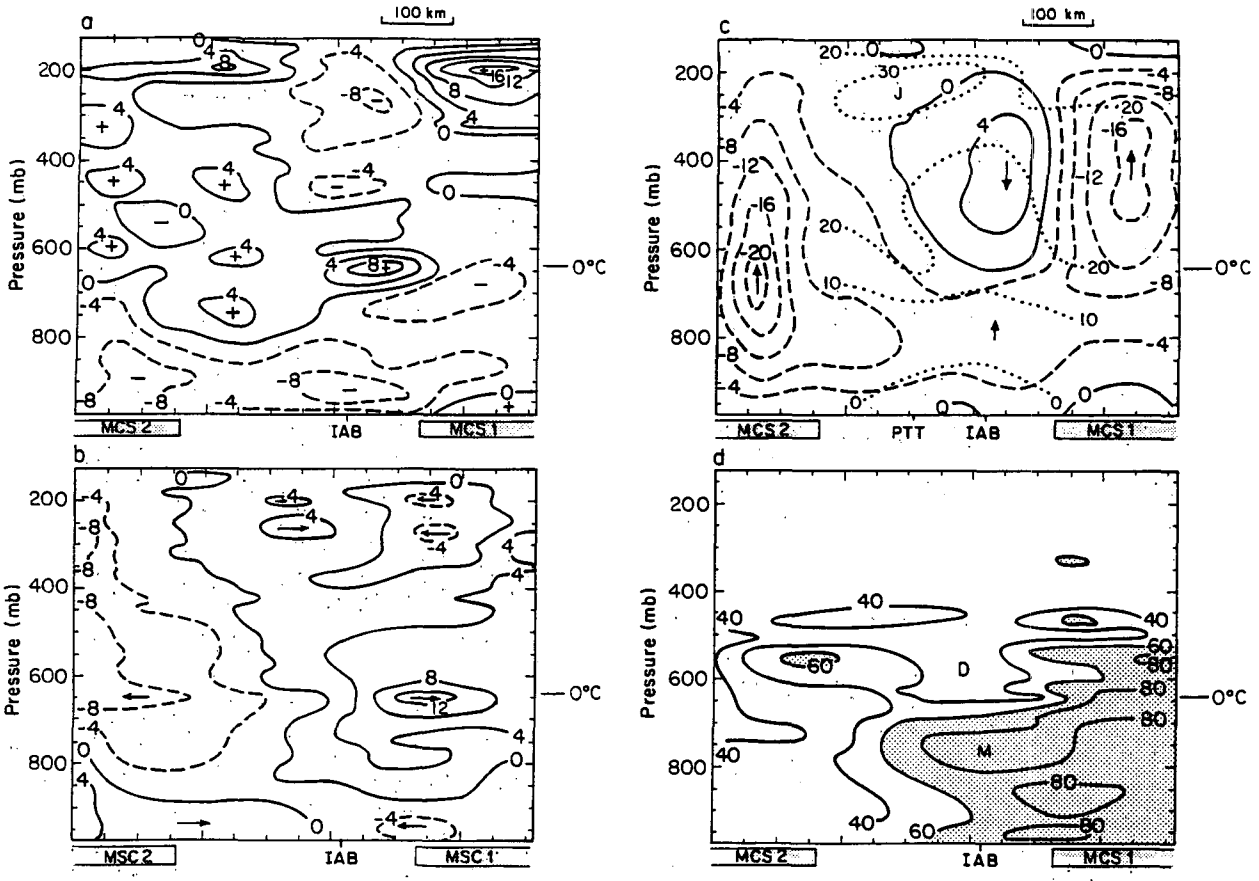

FIG. 14. Southwest–northeast vertical cross section along line segment in Fig. 9 intersecting MCS1 and MCS2 (bars at bottom) of (a) divergence (10^{-5} s^{-1}), (b) perturbation flow in the plane of the section (m s^{-1}), (c) vertical p velocity (10^{-3} mb s^{-1}), and isotachs (m s^{-1}; dotted lines; J marks jet core) for flow perpendicular to the section, and (d) relative humidity (%; values greater than 60% shaded) at 0000 UTC 15 June 1985. Wet-bulb temperature T_w = 0°C level is indicated.

prior to 0000 for this subsidence to reach the midpoint. It is possible that MCS1 contributed more to the subsidence at IAB since it was more mature at this time.

The relative humidity field (Fig. 14d), showing dry air above IAB and moist air below, is consistent with the pattern of subsidence aloft and ascent at low levels. Deep moisture is evident in the region of MCS1 but not MCS2. The lack of low-level moistening associated with MCS2 is most likely an artifact of missing sounding data in the area of convective development.

Soundings for IAB and PTT (Pratt) at 0000 show the effects of subsidence aloft with sharp temperature and moisture inversions between 650 and 700 mb (Figs. 15a and 15b).[4] The temperature and moisture inversions were sharper at IAB, near the center of the "gap," than at PTT. The changes in the IAB sounding over the 3-h period from 2100 on 14 June to 0000 (Fig. 15a)—cooling and moistening below 670 mb and warming and drying above—are consistent with the pattern of vertical motion—ascent below descent—shown in Fig. 14c. The primary change at PTT from 2100 to 0000 was a cooling and moistening below 700 mb. Changes aloft were minor, consistent with the weak vertical motion field over PTT at this time (Fig. 14c). It appears from the moistening and cooling below the inversions that low-level ascent was a dominant factor in elevating the earlier inversions near 750–800 mb.

The IAB and PTT soundings clearly show why no *deep* convection developed in the gap despite low-level upward motion. The surface convective temperatures needed to break the strong inversions were 40° and 36°C, respectively, whereas observed temperatures at 0000 did not exceed 30°C (Fig. 8a). However, reference to the 2100 soundings (Fig. 15) indicates that even at 2100, there was considerable convective inhibition (CIN, Colby 1984) present prior to any significant MCS-produced modifications. Therefore, convec-

[4] Stensrud and Maddox (1988) used a one-dimensional model to demonstrate that the warming and drying aloft beneath the converging outflows in the 23–24 June case could be explained almost entirely as a result of vertical rather than horizontal motions.

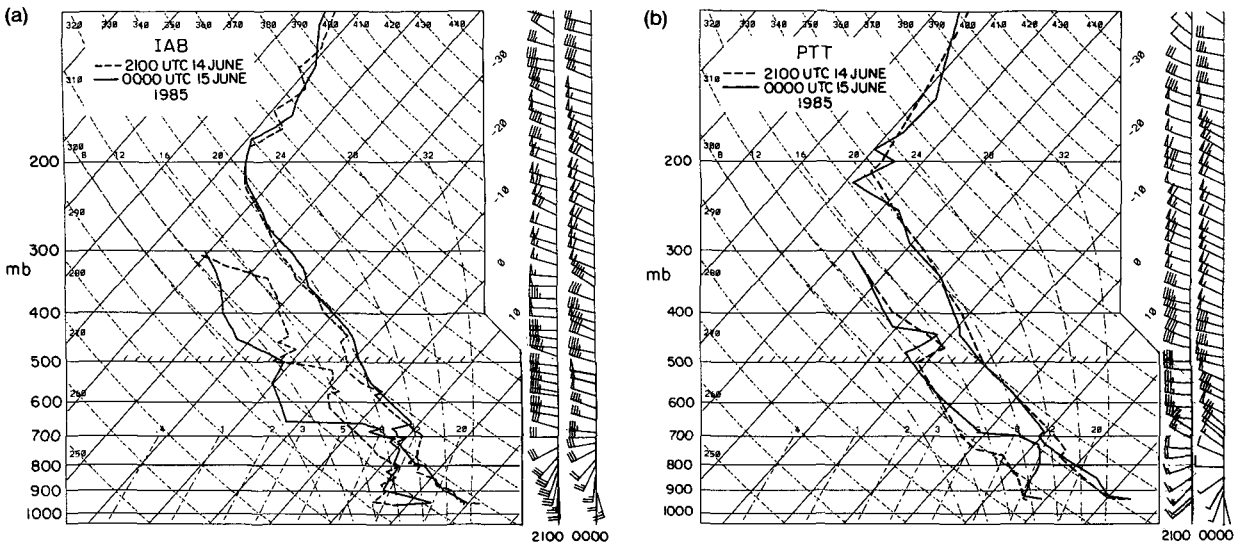

FIG. 15. Soundings from (a) Wichita (IAB) and (b) Pratt (PTT) at 2100 UTC 14 June (dashed) and 0000 UTC 15 June (solid).

tion was unlikely to develop in this region regardless, had conditions aloft remained unchanged. On the other hand, had the upward motion evident at 2100 in the gap (Fig. 13) persisted, it would have weakened the cap and likely permitted convection to develop. The reversal from upward to downward motion in the gap from 2100 to 0000 kept CIN large and restricted deep convection. Farther along the front to the southwest, however, surface temperatures exceeded 36°C (Fig. 3). No soundings were available in this region, but assuming they were similar to those at PTT and IAB, convective temperatures would have been reached, thereby accounting for the development of MCS2 in that location.

As noted earlier, the gap persisted well beyond 0000, but diagnosis of divergence and vertical motion at later times was hindered by missing sounding data. To illustrate this problem, divergence fields at the surface and 200 mb at 0300 are shown in Figs. 16 and 17, respectively. At the surface, convergence was still present along

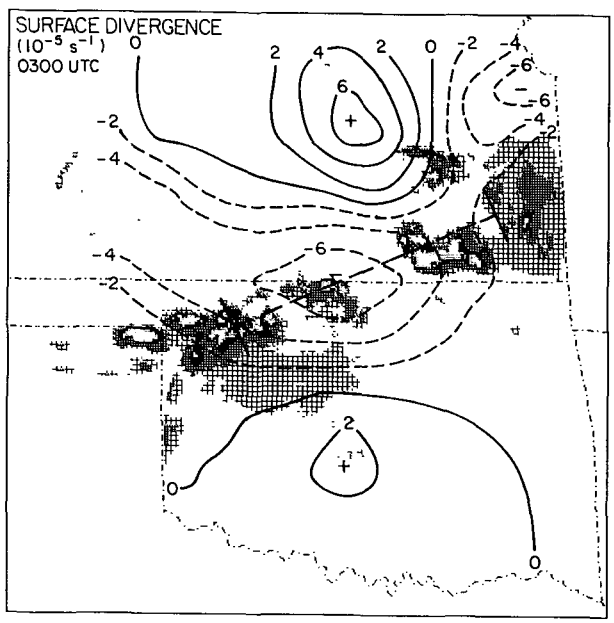

FIG. 16. Surface divergence (10^{-5} s^{-1}) and radar reflectivity at 0300 UTC 15 June 1985. Dashed straight-line segment is center axis of cross section shown in Fig. 18. Reflectivity thresholds are 16, 25, 40, and 49 dBZ.

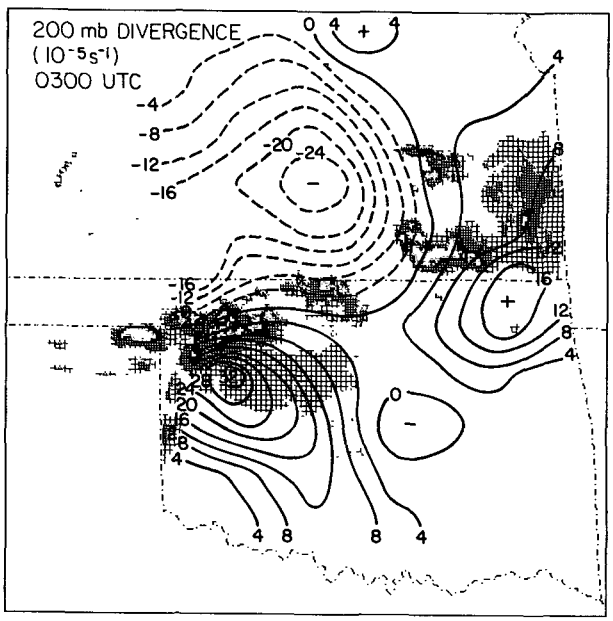

FIG. 17. As in Fig. 16 except at 200 mb.

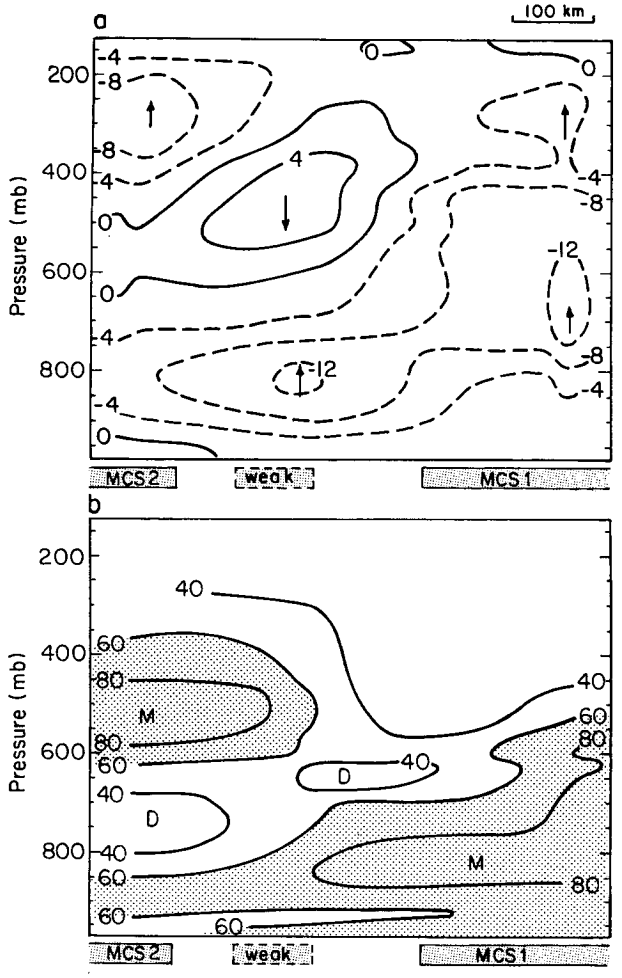

FIG. 18. Southwest–northeast vertical cross section along line segment shown in Fig. 16 intersecting MCS1, MCS2, and weak convection between (shaded bars at bottom) of (a) vertical p velocity (10^{-3} mb s^{-1}) and (b) relative humidity (%) at 0300 UTC 15 June 1985.

the front with some of the largest values in the region of the gap. At 200 mb, strong divergence centers were associated with each MCS, while a region of convergence existed between the two and behind the line. The vertical motion pattern along a 100-km-wide band centered on the line segment shown in Fig. 16 supports this finding (Fig. 18a). It shows sinking motion aloft and rising motion below 600 mb in the area of the gap; however, there are some inconsistencies (e.g., a region of sinking motion at midlevels that extends into the area of MCS2). This unrealistic result is a consequence of the Woodward (WWR) sounding, within MCS2 at this time, terminating at 580 mb (Fig. 19). This sounding partly resembles the so-called onion-type structure found to be characteristic of soundings ascending into upper-level stratiform clouds (Zipser 1977). It contains evidence of strong sinking in the lower troposphere in a mesoscale downdraft. The sounding at Chanute (CNU) also as-

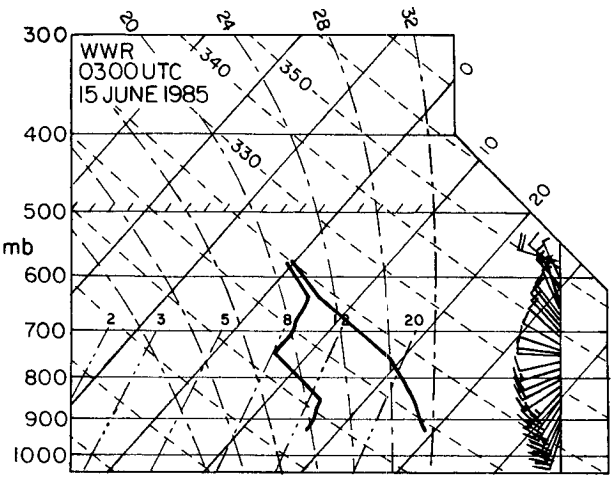

FIG. 19. Sounding from Woodward (WWR) at 0300 UTC 15 June 1985.

cended into active convection and terminated early (at 470 mb), thereby complicating the interpretation of the diagnosed fields near MCS1. The moisture field, characterized by dry conditions aloft and moist conditions at low levels in the region of the gap (Fig. 18b), was similar to that at 0000 as the front passed Wichita (Fig. 14d) and is again consistent with sinking aloft and ascent at low levels.

5. The squall-line gap

a. Vertical cross section

A schematic of the precipitation and circulation patterns along the squall line at the time of the gap at Wichita

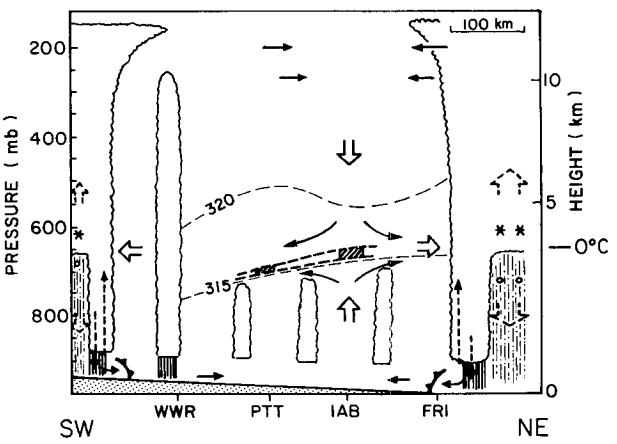

FIG. 20. Schematic of cloud field, inversion structure, and airflow along cold front at 0000 UTC 15 June 1985. Solid arrows represent flow determined by sounding data; dashed arrows represent hypothesized flow. Cloud boundaries are estimated from radar and photographic data. Thick dashed lines represent inversion layer based on inversions at IAB and PTT (hatched regions). Thin dashed lines are isentropes (K). Wet-bulb temperature T_w = 0°C is indicated. Barbed symbols at bottom are gust fronts.

is shown in Fig. 20. Locations of the MCSs are based on radar data, although details of their internal structure could not be determined and are, therefore, hypothetical. Congestus clouds in the vicinity of IAB were photographed by one of us (RJ). Horizontal divergence near the melting level over IAB was collocated with a sharp inversion, which sloped downward slightly toward PTT along the 315-K isentrope. From thermal wind considerations, this slope is consistent with increasing northwesterly flow with height in this layer (Fig. 15).

The approximate collocation of the inversion in the squall-line gap with the melting level does not appear to be a coincidence. Analyses of sounding data from the recent TOGA COARE (Tropical Ocean Global Atmosphere Coupled Ocean–Atmosphere Response Experiment, November 1992–February 1993) have revealed frequent occurrences of temperature inversions near the 0°C level in the environment of convective systems (Hart et al. 1994). A similar finding for the eastern Pacific has been reported by Haraguchi (1968). It is well known that melting *within* stratiform cloud layers can produce an isothermal layer there (Findeisen 1940). However, Nicholls et al. (1991) have shown that gravity waves forced by a vertical distribution of heating containing the effects of melting (a strong vertical gradient of heating in the midtroposphere) tend to produce a stable region in the midtroposphere *outside* the region of the heat source. Melting has also been shown to induce horizontal wind perturbations such as observed here (Atlas et al. 1969; Lin and Stewart 1986; Szeto et al. 1988; Nicholls et al. 1991). The jetlike structure of the horizontal inflow into the MCSs (Fig. 14b) coincident with the inversion may be a result of the stable layer allowing large shears to develop. It is interesting to note that the positioning of the inversion near the 0°C level prevented the congestus in the gap region from glaciating and realizing additional buoyancy for growth from the latent heat of fusion.

The strong CIN along the front explains why a continuous line of convection did not form all along it. Strong low-level convergence was everywhere present, but convection formed only where the cap was either weak or could be overcome by strong surface heating (in the case of MCS2) or by lifting (e.g., due to upper-level jet forcing). Subsequent perturbations to the flow in the gap kept CIN large and prevented deep convection from breaking out. Many squall lines, of course, contain a contiguous band of deep convective cells. In those cases (e.g., the 10–11 June PRE-STORM squall line) the CIN is weak and convergence at the wind shift line can readily generate deep convection all along it.

b. A Wichita gap?

Can an argument be advanced for a preferential splitting of squall lines at Wichita? Certainly not from the limited time record of PRE-STORM data. The two PRE-STORM cases of this phenomenon documented so far, both involving northeast–southwest-oriented cold fronts propagating across Kansas and Oklahoma, have several commonalities, but it is inappropriate to generalize from just two cases.

In the 14–15 June event, triggering of convection along the western portion of the cold front first occurred over the elevated terrain of the Raton Mesa in southeastern Colorado (Fig. 7). In the 23–24 June case, convection was initiated along a dryline in western Kansas (Johnson et al. 1989). Prior to the western MCS development in both cases, prominent MCSs developed in northeastern Kansas where the cold front was particularly strong. If along cold fronts such as these (which appear to be common during spring and summer) the initiation of an MCS is favored in western Kansas and Oklahoma due to elevated heating or dryline-triggering mechanisms *and* another MCS develops well to the northeast (for whatever reason), then a gap may be favored over central Kansas. However, without a climatological study involving many years of radar, satellite, and other data, any conclusions drawn on this matter must be regarded as highly speculative.

6. Summary and conclusions

Two mesoscale convective systems developed along a cold front traversing Kansas and Oklahoma on 14–15 June 1985. The two storms remained separated throughout their lifetimes and eventually grew to MCC (Maddox 1980) proportions. Strong low-level convergence between the two (in the vicinity of Wichita, Kansas), along with abundant moisture, portended the formation of new deep convection in the region. However, deep convection did not develop. Computations of vertical velocity showed that low-level vertical motion was indeed upward within the gap; however, strong subsidence existed aloft. The demarcation between subsidence aloft and ascent at low levels was near the melting level, where there was a concurrent inflow into the MCSs. A strong inversion existed there, which effectively capped congestus clouds in the squall-line gap. Similar temperature inversions near the melting level have been reported in the Tropics (Haraguchi 1968; Hart et al. 1994).

It appears as though the pattern of convection along the front (which was oriented perpendicular to an upper-level jet streak) was influenced both by jet streak secondary circulations and convectively generated flows. Convection first developed in the left-exit region of the jet streak, consistent with expected forcing by jet streak secondary circulations (Namais and Clapp 1949; Uccellini and Johnson 1979; Keyser and Shapiro 1986). Shortly thereafter, convection developed approximately 500 km to the southwest over higher terrain in western Kansas and Oklahoma (in the right-exit region of jet), likely as a result of strong surface heating. A strong cap existed in the region of the gap prior to the maturing of both MCSs. During this early stage,

the jet streak appeared to be forcing deep upward motion there, which should have served to weaken the cap; however, in just 3 h the vertical motion in the gap reverted to downward at upper levels as the convection developed in the MCSs—leading to a continued inhibition of convection in the region.

As the two MCSs developed further, circulations between the two became significantly perturbed. These circulations resembled those observed elsewhere in the Tropics and midlatitudes and are consistent with those expected outside an MCS-like convective heat source due to thermally forced gravity waves (e.g., Nicholls et al. 1991; Mapes 1993). Surface and upper-level outflows and midlevel inflows are induced by heat sources characteristic of the stratiform components of MCSs. Such flow features were observed in connection with both MCSs in the 14–15 June 1985 case. Increased stability develops in the midtroposphere following the passage of the convectively generated gravity waves or buoyancy bores (after Mapes 1993) owing to net vertical displacements arising from the net heating. Recent numerical computations by Pandya et al. (1993) indicate that despite vertical energy propagation, considerable energy remains in the second internal ($n = 2$) mode within several hundred kilometers of the heat source, supporting the findings of Nicholls et al. (1991) and Mapes (1993). Therefore, the rising and strengthening of the inversion near the 0°C level in the squall-line gap can be qualitatively explained by the action of such gravity waves.

The degree to which gravity wave theory can fully account for the observed atmospheric structure in the gap is uncertain, owing to other complicating factors (e.g., unknown heating distributions and their time dependence, mean flow, and Coriolis effects). Moreover, gravity wave effects are likely superposed upon jet streak secondary circulations. A possible way of separating the two is to examine the dynamic and diabatic contributions to the ageostrophic cross-jet motion (e.g., Uccellini and Johnson 1979; Keyser and Johnson 1984; Sortais et al. 1993); however, the relatively sparse sounding data would require the application of a mesoscale numerical model for this purpose.

PRE-STORM researchers and forecasters in the Wichita area, on this day, marveled at the strong low-level forcing and the growth of vigorous congestus in the area of the gap, but there was a lack of deep convective development. As Stensrud and Maddox (1988) have pointed out, situations such as this, with strongly opposing flows in the environment of MCSs, present one of the most challenging convective forecasting problems.

The gap between the two large MCSs observed in this case appears to be quite distinct from smaller gaps between individual thunderstorm cells along a nearly contiguous squall line. Squall lines of the latter type frequently occur when there is relatively weak convective inhibition (CIN) in the presence of strong low-level convergence along fronts, wind shift lines, or gust fronts. The common occurrence of thunderstorm cell or small-scale squall-line gaps in the latter cases [noted in the climatologies of Bluestein and Jain (1985) and Houze et al. (1990)] may at times be related to interfering outflows aloft but are more often probably connected with surface effects such as gust front surges, pressure perturbations, inhomogeneities along the line, etc. In cases of gaps between MCSs, the conventional sounding network is too coarse to sample these events, although the NWS Wind Profiler Demonstration Network may be adequate in some cases. Whether or not there are preferred sites for squall-line gaps, regardless of their scale, is an open question. The resolution of this issue will have to await the results of comprehensive radar analyses.

Acknowledgments. The assistance of Rick Taft, Bill Gallus, Bob Falvey, Xin Lin, and Scot Loehrer in the analysis effort and discussions with Mel Nicholls, Wayne Schubert, Brian Mapes, Jim Bresch, and Greg Holland are greatly appreciated. Thanks are also extended to José Meitín and Robert Hueftle of NOAA for their help in preparing the composite radar analyses. This research has been supported by the National Science Foundation, Atmospheric Sciences Division, under Grants ATM-9013112 and ATM-9313716.

REFERENCES

Atlas, D., R. Tatehira, R. C. Srivastava, W. Marker, and R. E. Carbone, 1969: Precipitation-induced mesoscale wind perturbations in the melting layer. *Quart. J. Roy. Meteor. Soc.*, **95,** 544–560.

Augustine, J. A., and K. W. Howard, 1988: Mesoscale convective complexes of the United States during 1985. *Mon. Wea. Rev.*, **116,** 685–701.

Barnes, S. L., 1964: A technique for maximizing details in numerical weather map analysis. *J. Appl. Meteor.*, **3,** 396–409.

Biggerstaff, M. I., and R. A. Houze Jr., 1991: Kinematic and precipitation structure of the 10–11 June 1985 squall line. *Mon. Wea. Rev.*, **119,** 3034–3065.

Bjerknes, J., 1938: Saturated adiabatic ascent of air through a dry-adiabatically descending environment. *Quart. J. Roy. Meteor. Soc.*, **108,** 325–330.

Bluestein, H. B., and M. H. Jain, 1985: Formation of mesoscale lines of precipitation: Severe squall lines in Oklahoma during the spring. *J. Atmos. Sci.*, **42,** 1711–1732.

Bretherton, C. S., and P. K. Smolarkiewicz, 1989: Gravity waves, compensating subsidence and detrainment around cumulus clouds. *J. Atmos. Sci.*, **46,** 740–759.

Byers, H. R., and R. R. Braham, 1949: *The Thunderstorm.* U.S. Govt. Printing Office, Washington DC, 287 pp. [NTIS PB-234-515.]

Carbone, R. E., 1982: A severe frontal rainband. Part I: Stormwide hydrodynamic structure. *J. Atmos. Sci.*, **39,** 258–279.

Chong, M., P. Amayenc, G. Scialom, and J. Testud, 1987: A tropical squall line observed during the COPT 81 experiment in west Africa. Part I: Kinematic structure inferred from dual-Doppler radar data. *Mon. Wea. Rev.*, **115,** 670–694.

Colby, F. P., Jr., 1984: Convective inhibition as a predictor of convection during AVE-SESAME II. *Mon. Wea. Rev.*, **112,** 2239–2252.

Cunning, J. B., 1986: The Oklahoma–Kansas Preliminary Regional Experiment for STORM-Central. *Bull. Amer. Meteor. Soc.*, **67,** 1478–1486.

Findeisen, W., 1940: The formation of the 0°C isothermal layer and fractocumulus under nimbostratus. *Meteor. Z.*, **57,** 49–54.

Fritsch, J. M., 1975: Cumulus dynamics: Local compensating subsidence and its implications for cumulus parameterization. *Pure Appl. Geophys.*, **113,** 851–867.

——, and C. G. Chappell, 1980: Numerical prediction of convectively driven mesoscale pressure systems. Part II: Mesoscale model. *J. Atmos. Sci.*, **37,** 1734–1762.

Gallus, W. A., Jr., and R. H. Johnson, 1991: Heat and moisture budgets of an intense midlatitude squall line. *J. Atmos. Sci.*, **48,** 122–146.

——, and ——, 1992: The momentum budget of an intense midlatitude squall line. *J. Atmos. Sci.*, **49,** 422–450.

Gamache, J. F., and R. A. Houze Jr., 1982: Mesoscale air motions associated with a tropical squall line. *Mon. Wea. Rev.*, **10,** 118–135.

Haraguchi, P. Y., 1968: Inversions over the tropical eastern Pacific Ocean. *Mon. Wea. Rev.*, **96,** 177–185.

Hart, K. A., R. H. Johnson, and P. E. Ciesielski, 1994: Tropical water vapor distributions measured in TOGA/COARE. Preprints, *Ninth Conference on Climate Variations,* Nashville, TN, Amer. Meteor. Soc., J48–J52.

Houze, R. A., Jr., and E. N. Rappaport, 1984: Air motions and precipitation structure of an early summer squall line over the eastern tropical Atlantic. *J. Atmos. Sci.*, **41,** 553–574.

——, B. F. Smull, and P. Dodge, 1990: Mesoscale organization of spring-time rainstorms in Oklahoma. *Mon. Wea. Rev.*, **118,** 613–654.

Hoxit, L. R., C. F. Chappell, and J. M. Fritsch, 1976: Formation of mesolows or pressure troughs in advance of cumulonimbus clouds. *Mon. Wea. Rev.*, **104,** 1419–1428.

Johnson, R. H., 1982: Vertical motion in near-equatorial winter monsoon convection. *J. Meteor. Soc. Japan,* **60,** 682–689.

——, and P. J. Hamilton, 1988: The relationship of surface pressure features to the precipitation and air flow structure of an intense midlatitude squall line. *Mon. Wea. Rev.*, **116,** 1444–1472.

——, S. Chen, and J. J. Toth, 1989: Circulations associated with a mature-to-decaying midlatitude mesoscale convective system. Part I: Surface features—Heat bursts and mesolow development. *Mon. Wea. Rev.*, **117,** 945–959.

Keyser, D. A., and D. R. Johnson, 1984: Effects of diabatic heating on the ageostrophic circulation of an upper tropospheric jet streak. *Mon. Wea. Rev.*, **112,** 1709–1724.

——, and M. A. Shapiro, 1986: A review of the structure and dynamics of upper-level frontal zones. *Mon. Wea. Rev.*, **114,** 452–498.

Kocin, P. J., L. W. Uccellini, and R. A. Peterson, 1986: Rapid evolution of a jet streak circulation in a pre-convective environment. *Meteor. Atmos. Phys.*, **35,** 103–138.

Leary, C. A., and R. A. Houze Jr., 1979: Melting and evaporation of hydrometeors in precipitation from the anvil clouds of deep tropical convection. *J. Atmos. Sci.*, **36,** 669–679.

Lilly, D. K., 1960: On the theory of disturbances in a conditionally unstable atmosphere. *Mon. Wea. Rev.*, **88,** 1–17.

Lin, C. A., and R. E. Stewart, 1986: Mesoscale circulations initiated by melting snow. *J. Geophys. Res.*, **91,** 13 299–13 302.

Loehrer, S. M., 1992: The surface pressure features and precipitation structure of PRE-STORM mesoscale convective systems. Atmos. Sci. Paper No. 518, Colorado State University, 297 pp. [Available from the author at Dept. of Atmospheric Science, Colorado State University, Fort Collins, CO 80523.]

Maddox, R. A., 1980: Mesoscale convective complexes. *Bull. Amer. Meteor. Soc.*, **61,** 1374–1387.

——, 1983: Large-scale meteorological conditions associated with midlatitude, mesoscale convective complexes. *Mon. Wea. Rev.*, **111,** 1475–1493.

Mapes, B. E., 1993: Gregarious tropical convection. *J. Atmos. Sci.*, **50,** 2026–2037.

——, and R. A. Houze Jr., 1993: An integrated view of the 1987 Australian monsoon and its mesoscale convective systems. *Quart. J. Roy. Meteor. Soc.*, **119,** 733–754.

Namias, J., and P. F. Clapp, 1949: Confluence theory of the high tropospheric jet-stream. *J. Meteor.*, **6,** 330–336.

Nicholls, M. E., R. A. Pielke, and W. R. Cotton, 1991: Thermally forced gravity waves in an atmosphere at rest. *J. Atmos. Sci.*, **48,** 1869–1884.

O'Brien, J. J., 1970: Alternative solutions to the classical vertical velocity problem. *J. Appl. Meteor.*, **9,** 197–203.

Ogura, Y., and M. T. Liou, 1980: The structure of a mid-latitude squall line. A case study. *J. Atmos. Sci.*, **37,** 553–567.

Pandya, R., D. Durran, and C. Bretherton, 1993: Comments on "Thermally forced gravity waves in an atmosphere at rest." *J. Atmos. Sci.*, **50,** 4097–4101.

Purdom, J. F. W., and K. Marcus, 1982: Thunderstorm trigger mechanisms over the southeast United States. Preprints, *12th Conference of Severe Local Storms,* San Antonio, TX, Amer. Meteor. Soc., 487–488.

Shapiro, M. A., 1981: Frontogenesis and geostrophically forced secondary circulations in the vicinity of jet stream–frontal zone systems. *J. Atmos. Sci.*, **38,** 954–973.

Simpson, J. S., N. E. Westcott, R. J. Clerman, and R. A. Pielke, 1980: On cumulus mergers. *Arch. Meteor. Geophys. Bioklimatol. Ser. A.*, **29,** 1–40.

Smull, B. F., and R. A. Houze Jr., 1987: Rear inflow in squall lines with trailing stratiform precipitation. *Mon. Wea. Rev.*, **115,** 2869–2889.

Sortais, J.-L., J.-P. Cammas, X. D. Yu, E. Richard, and R. Rossett, 1993: A case study of coupling between low- and upper-level front systems: Investigation of dynamical and diabatic processes. *Mon. Wea. Rev.*, **121,** 2239–2253.

Stensrud, D. J., and R. A. Maddox, 1988: Opposing mesoscale circulations: A case study. *Wea. Forecasting,* **3,** 189–204.

Szeto, K. K., C. A. Lin, and R. E. Stewart, 1988: Mesoscale circulations forced by melting snow. Part I: Basic simulations and dynamics. *J. Atmos. Sci.*, **45,** 1629–1641.

Toth, J. J., 1987: Interaction of shallow cold surges with topography on scales of 100–1000 kilometers. Cooperative Institute for Research in the Atmosphere Paper, Colorado State University, Fort Collins, CO, 135 pp.

Uccellini, L. W., and D. R. Johnson, 1979: The coupling of upper and lower jet streaks and implications for the development of severe convective storms. *Mon. Wea. Rev.*, **107,** 682–703.

Weaver, J. F., and S. P. Nelson, 1982: Multiscale aspects of thunderstorm gust fronts and their effects on subsequent storm development. *Mon. Wea. Rev.*, **110,** 707–718.

Wilson, J. W., and W. E. Schreiber, 1986: Initiation of convective storms at radar-observed boundary-layer convergence lines. *Mon. Wea. Rev.*, **114,** 2516–2536.

Zipser, E. J., 1977: Mesoscale and convective-scale downdrafts as distinct components of squall-line circulation. *Mon. Wea. Rev.*, **105,** 1568–1589.